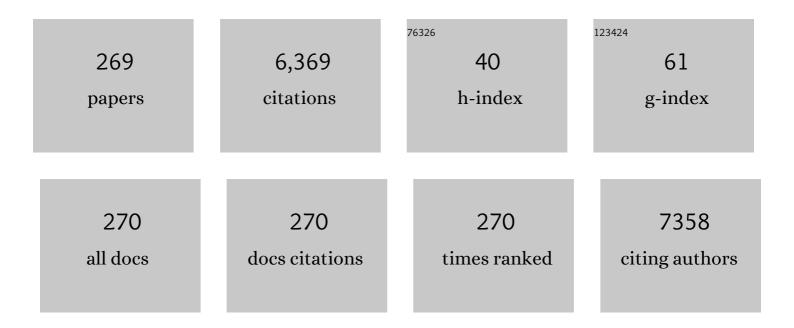
List of Publications by Year in descending order

Source: https://exaly.com/author-pdf/183583/publications.pdf Version: 2024-02-01



YONG-ULLEE

#	Article	IF	CITATIONS
1	Recent advances in fluorescent upconversion nanomaterials: novel strategies for enhancing optical and magnetic properties to biochemical sensing and imaging applications. Applied Spectroscopy Reviews, 2022, 57, 265-299.	6.7	14
2	Synthesis of Magnetically Recoverable Ru/Fe3O4 Nanocomposite for Efficient Photocatalytic Degradation of Methylene Blue. Journal of Cluster Science, 2022, 33, 853-865.	3.3	11
3	Optical properties of Sr2YF7 material doped with Yb3+, Er3+, and Eu3+ ions for solar cell application. Journal of Alloys and Compounds, 2022, 897, 163189.	5.5	14
4	Studies on Synthesis and Characterization of Fe <sub>3</sub> O <sub>4</sub> @SiO <sub>2</sub> @Ru Hybrid Magnetic Composites for Reusable Photocatalytic Application. Adsorption Science and Technology, 2022, 2022, .	3.2	9
5	A review on graphene quantum dots, an emerging luminescent carbon nanolights: Healthcare and Environmental applications. Materials Science and Engineering B: Solid-State Materials for Advanced Technology, 2022, 278, 115633.	3.5	14
6	Water-stable perovskite-loaded nanogels containing antioxidant property for highly sensitive and selective detection of roxithromycin in animal-derived food products. Scientific Reports, 2022, 12, 3147.	3.3	9
7	Self-Assembly of Polystyrene- <i>b</i> -poly(2-vinylpyridine)/Chloroauric Acid at the Liquid/Liquid Interface. Langmuir, 2022, , .	3.5	6
8	Magnetic visible-light activated photocatalyst ZnFe2O4/BiVO4/g-C3N4 for decomposition of antibiotic lomefloxacin: Photocatalytic mechanism, degradation pathway, and toxicity assessment. Chemosphere, 2022, 299, 134320.	8.2	29
9	Recent advances in turn off-on fluorescence sensing strategies for sensitive biochemical analysis - A mechanistic approach. Microchemical Journal, 2022, 179, 107511.	4.5	24
10	Solventâ€resistant microfluidic paperâ€based analytical device/spray mass spectrometry for quantitative analysis of C <sub>18</sub> â€ceramide biomarker. Journal of Mass Spectrometry, 2021, 56, e4611.	1.6	10
11	Patterning microporous paper with highly conductive silver nanoparticles <i>via</i> PVP-modified silver–organic complex ink for development of electric valves. Materials Advances, 2021, 2, 3579-3588.	5.4	6
12	Selective optosensing of iron(III) ions in HeLa cells using NaYF4:Yb3+/Tm3+ upconversion nanoparticles coated with polyepinephrine. Analytical and Bioanalytical Chemistry, 2021, 413, 1363-1371.	3.7	10
13	Preparation, Properties, and Microbial Impact of Tungsten (VI) Oxide and Zinc (II) Oxide Nanoparticles Enriched Polyethylene Sebacate Nanocomposites. Polymers, 2021, 13, 718.	4.5	4
14	Large-Area Assembly of Metal–Organic Layered Ultrathin Films at the Liquid/Liquid Interface. Langmuir, 2021, 37, 4515-4522.	3.5	7
15	Highly sensitive and selective detection of Alprenolol using upconversion nanoparticles functionalized with amphiphilic conjugated polythiophene. Microchemical Journal, 2021, 164, 106010.	4.5	3
16	Simple fluorescence optosensing probe for spermine based on ciprofloxacin-Tb3+ complexation. PLoS ONE, 2021, 16, e0251306.	2.5	10
17	Amphiphilic Conjugated Polythiopheneâ€based Fluorescence " <i>Turn on</i> ―Sensor for Selective Detection of <scp><i>Escherichia coli</i></scp> in Water and Milk. Bulletin of the Korean Chemical Society, 2021, 42, 1047-1053.	1.9	5
18	Novel polyaniline/tungsten trioxide@metal–organic framework nanocomposites for enhancing photodegradation of 4-nitrophenol. Environmental Technology and Innovation, 2021, 22, 101404.	6.1	10

#	Article	IF	CITATIONS
19	Metabolic labeling of glycans with isotopic glucose for quantitative glycomics in yeast. Analytical Biochemistry, 2021, 621, 114152.	2.4	7
20	Visible light-activated NGQD/nsC3N4/Bi2WO6 microsphere composite for effluent organic matter treatment. Chemical Engineering Journal, 2021, 415, 129024.	12.7	19
21	Highly stable Cs4PbBr6/CsPbBr3perovskite nanoparticles as a new fluorescence nanosensor for selective detection of trace tetracycline in food samples. Journal of Industrial and Engineering Chemistry, 2021, 104, 437-444.	5.8	19
22	Ultrasensitive detection and removal of carbamazepine in wastewater using UCNPs functionalized with thin-shell MIPs. Microchemical Journal, 2021, 170, 106674.	4.5	14
23	Selective dual detection of Hg <sup>2+</sup> and TATP based on amphiphilic conjugated polythiophene-quantum dot hybrid materials. Analyst, The, 2021, 146, 2894-2901.	3.5	14
24	Recent Advances in Nanomicelles Delivery Systems. Nanomaterials, 2021, 11, 70.	4.1	55
25	Novel aspartic chiral optical sensor based on β-cyclodextrin-functionalized CdTe nanoparticles. Inorganic Chemistry Communication, 2021, 134, 109036.	3.9	5
26	Photocatalytic activity of Yb, Er, Ceâ€codoped TiO <sub>2</sub> for degradation of Rhodamine B and 4â€chlorophenol. Journal of Chemical Technology and Biotechnology, 2020, 95, 2664-2673.	3.2	10
27	ZnO-Bi2O3/graphitic carbon nitride photocatalytic system with H2O2-assisted enhanced degradation of Indigo carmine under visible light. Arabian Journal of Chemistry, 2020, 13, 3790-3800.	4.9	39
28	Highly selective and sensitive optosensing of glutathione based on fluorescence resonance energy transfer of upconversion nanoparticles coated with a Rhodamine B derivative. Arabian Journal of Chemistry, 2020, 13, 2671-2679.	4.9	15
29	Block copolymer vesicles via liquid/liquid interface-mediated self-assembly. Applied Surface Science, 2020, 499, 143896.	6.1	5
30	Paper-based colorimetric probe for highly sensitive detection of folic acid based on open-ring form amplification of rhodamine B derivative. Journal of Industrial and Engineering Chemistry, 2020, 81, 352-359.	5.8	20
31	Surface and morphology analyses, and voltammetry studies for electrochemical determination of cerium( <scp>iii</scp> ) using a graphene nanobud-modified-carbon felt electrode in acidic buffer solution (pH 4.0 ű 0.05). RSC Advances, 2020, 10, 37409-37418.	3.6	15
32	Inkjetâ€based microreactor for the synthesis of silver nanoparticles on plasmonic paper decorated with chitosan nanoâ€wrinkles for efficient onâ€site Surfaceâ€enhanced Raman Scattering (SERS). Nano Select, 2020, 1, 499-509.	3.7	10
33	Photoluminescence of Binary and Ternary Europiumâ€based Polyhedral Oligomeric Silsesquioxane and Sol–Gel Complexes. Bulletin of the Korean Chemical Society, 2020, 41, 782-785.	1.9	0
34	Dual emission nonionic molecular imprinting conjugated polythiophenes-based paper devices and their nanofibers for point-of-care biomarkers detection. Biosensors and Bioelectronics, 2020, 160, 112211.	10.1	51
35	Novel "turn on–off―paper sensor based on nonionic conjugated polythiophene-coated CdTe QDs for efficient visual detection of cholinesterase activity. Analyst, The, 2020, 145, 4305-4313.	3.5	22
36	H2O2-assisted photocatalysis for removal of natural organic matter using nanosheet C3N4-WO3 composite under visible light and the hybrid system with ultrafiltration. Chemical Engineering Journal, 2020, 399, 125733.	12.7	59

#	Article	IF	CITATIONS
37	Highly sensitive colorimetric paper-based analytical device for the determination of tetracycline using green fluorescent carbon nitride nanoparticles. Microchemical Journal, 2020, 158, 105151.	4.5	31
38	Highly sensitive and selective optosensing of quercetin based on novel complexation with yttrium ions. Analyst, The, 2020, 145, 3376-3384.	3.5	12
39	Novel reduced graphene oxide/ZnBi2O4 hybrid photocatalyst for visible light degradation of 2,4-dichlorophenoxyacetic acid. Environmental Science and Pollution Research, 2020, 27, 11127-11137.	5.3	21
40	Emerging spectroscopic techniques for prostate cancer diagnosis. Applied Spectroscopy Reviews, 2019, 54, 829-855.	6.7	1
41	Disposable Colorimetric Paper-Based Probe for the Detection of Amine-Containing Gases in Aquatic Sediments. ACS Omega, 2019, 4, 12665-12670.	3.5	16
42	Effects of hydrophobic/hydrophilic blocks ratio on PS-b-PAA self-assembly in solutions, in emulsions, and at the interfaces. Colloids and Surfaces A: Physicochemical and Engineering Aspects, 2019, 580, 123684.	4.7	9
43	Enhanced performance in the photocatalytic degradation of 2,4,5-Trichlorophenoxyacetic acid over Eu-doped Bi2WO6 under visible light irradiation. Korean Journal of Chemical Engineering, 2019, 36, 1716-1723.	2.7	17
44	Oxidation of sulfides including DBT using a new vanadyl complex of a nonâ€innocent <i>o</i> â€aminophenol benzoxazole based ligand. Applied Organometallic Chemistry, 2019, 33, e4781.	3.5	8
45	Fluorescence Optosensing of Triclosan by Upconversion Nanoparticles with Potassium Permanganate. ACS Omega, 2019, 4, 7931-7937.	3.5	7
46	A facile low-cost paper-based SERS substrate for label-free molecular detection. Sensors and Actuators B: Chemical, 2019, 291, 369-377.	7.8	68
47	PS-b-PAA/Cu two-dimensional nanoflowers fabricated at the liquid/liquid interface: A highly active and robust heterogeneous catalyst. Colloids and Surfaces A: Physicochemical and Engineering Aspects, 2019, 570, 377-385.	4.7	4
48	Compact Integration of TiO2 Nanoparticles into the Cross-Points of 3D Vertically Stacked Ag Nanowires for Plasmon-Enhanced Photocatalysis. Nanomaterials, 2019, 9, 468.	4.1	17
49	Visible light-activated degradation of natural organic matter (NOM) using zinc-bismuth oxides-graphitic carbon nitride (ZBO-CN) photocatalyst: Mechanistic insights from EEM-PARAFAC. Chemosphere, 2019, 224, 597-606.	8.2	30
50	Highly sensitive and selective fluorescent sensor for tetrabromobisphenol-A in electronic waste samples using molecularly imprinted polymer coated quantum dots. Microchemical Journal, 2019, 144, 93-101.	4.5	51
51	Colorimetric detection of chromium(VI) using graphene oxide nanoparticles acting as a peroxidase mimetic catalyst and 8-hydroxyquinoline as an inhibitor. Mikrochimica Acta, 2019, 186, 36.	5.0	42
52	Highly selective and sensitive detection of catecholamines using NaLuGdF4:Yb3+/Er3+ upconversion nanoparticles decorated with metal ions. Sensors and Actuators B: Chemical, 2019, 284, 172-178.	7.8	28
53	Multiple Emitting Amphiphilic Conjugated Polythiophenes oated CdTe QDs for Picogram Detection of Trinitrophenol Explosive and Application Using Chitosan Film and Paperâ€Based Sensor Coupled with Smartphone. Advanced Science, 2019, 6, 1801467.	11.2	64
54	Recent advances on amphiphilic polymer-based fluorescence spectroscopic techniques for sensing and imaging. Applied Spectroscopy Reviews, 2019, 54, 204-236.	6.7	17

#	Article	IF	CITATIONS
55	Rare-earth free sensitizer in NaLuCrF4:Er upconversion material. Journal of Rare Earths, 2019, 37, 345-349.	4.8	5
56	Preparing cuprous oxide nanomaterials by electrochemical method for non-enzymatic glucose biosensor. Nanotechnology, 2018, 29, 205501.	2.6	23
57	A rapid and sensitive molecularly imprinted electrochemiluminescence sensor for Azithromycin determination in biological samples. Journal of Electroanalytical Chemistry, 2018, 813, 1-8.	3.8	30
58	A novel amphiphilic pH-responsive AlEgen for highly sensitive detection of protamine and heparin. Sensors and Actuators B: Chemical, 2018, 261, 233-240.	7.8	27
59	One-step synthesis of NaLu80â^'xGdxF4:Yb183+/Er23+(Tm3+) upconversion nanoparticles for in vitro cell imaging. Materials Science and Engineering C, 2018, 86, 56-61.	7.3	19
60	Iron(III) Amine Bis(phenolate) Complex Immobilized on Silicaâ€Coated Magnetic Nanoparticles: A Highly Efficient Catalyst for the Oxidation of Alcohols and Sulfides. ChemCatChem, 2018, 10, 1889-1899.	3.7	29
61	Fabricating highly catalytically active block copolymer/metal nanoparticle microstructures at the liquid/liquid interface. Journal of Colloid and Interface Science, 2018, 522, 272-282.	9.4	13
62	Photoluminescence spectroscopy of Cd-based quantum dots for optosensing biochemical molecules. Applied Spectroscopy Reviews, 2018, 53, 313-332.	6.7	11
63	Highly selective and sensitive fluorogenic ferric probes based on aggregation-enhanced emission with â" SiMe3 substituted polybenzene. Spectrochimica Acta - Part A: Molecular and Biomolecular Spectroscopy, 2018, 188, 202-207.	3.9	2
64	Enhanced fluorescence of CdTe quantum dots capped with a novel nonionic alginate for selective optosensing of ibuprofen. Sensors and Actuators B: Chemical, 2018, 256, 243-250.	7.8	36
65	Naturally modified nonionic alginate functionalized upconversion nanoparticles for the highly efficient targeted pH-responsive drug delivery and enhancement of NIR-imaging. Journal of Industrial and Engineering Chemistry, 2018, 57, 424-435.	5.8	39
66	Novel "turn off-on―sensors for highly selective and sensitive detection of spermine based on heparin-quenching of fluorescence CdTe quantum dots-coated amphiphilic thiophene copolymers. Sensors and Actuators B: Chemical, 2018, 257, 734-744.	7.8	46
67	Preface: Special issue on Nanopia 2016. Applied Spectroscopy Reviews, 2018, 53, 87-90.	6.7	0
68	Quantitative Analysis of Artificial Sweeteners by Capillary Electrophoresis with a Dualâ€Capillary Design of Molecularly Imprinted Solidâ€Phase Extractor. Bulletin of the Korean Chemical Society, 2018, 39, 1315-1319.	1.9	10
69	Enantioselective analysis of ketoprofen in human saliva by liquid chromatography/tandem mass spectrometry with chiral derivatization. Microchemical Journal, 2018, 143, 280-285.	4.5	6
70	Determination of N -glycans in glycoproteins using chemoenzymatic labeling with Endo-M N175Q. Microchemical Journal, 2017, 130, 390-399.	4.5	1
71	Influence of Cr3+ on upconversion luminescent and magnetic properties of NaLu0.86-xGd0.12F4:Crx3+/Er0.023+ (0≤â‰0.24) material. Journal of Luminescence, 2017, 187, 40-45.	3.1	20
72	Yb 3+ ,Er 3+ ,Eu 3+ -codoped YVO 4 material for bioimaging with dual mode excitation. Materials Science and Engineering C, 2017, 75, 990-997.	7.3	20

#	Article	IF	CITATIONS
73	A facile preparation of highly fluorescent carbon nitride nanoparticles via solid state reaction for optosensing mercury ions and bisphenol A. Microchemical Journal, 2017, 134, 13-18.	4.5	11
74	Development of a simple method for sensing melamine by SERS effect of Ag particles. Journal of Luminescence, 2017, 188, 436-440.	3.1	18
75	In situ generated Pb nanoclusters on basic lead carbonate ultrathin nanoplates as an effective heterogeneous catalyst. CrystEngComm, 2017, 19, 2860-2869.	2.6	13
76	Surface-enhanced Raman scattering using monolayer graphene-encapsulated Ag nanoparticles as a substrate for sensitive detection of 2,4,6-trinitrotoluene. Analytical Methods, 2017, 9, 3105-3113.	2.7	18
77	Enhanced light harvesting with chromium in NaLu0.70â^²xGd0.10F4:Yb0.18Er0.02Crx (0 ≤ ≤0.25) upconversion system. Materials Science and Engineering B: Solid-State Materials for Advanced Technology, 2017, 223, 91-97.	3.5	20
78	Enhanced photodegradation of 2,4-dichlorophenoxyacetic acid using a novel TiO2@MgFe2O4 core@shell structure. Chemosphere, 2017, 184, 849-856.	8.2	30
79	A Mixedâ€Metal Oxides/Graphitic Carbon Nitride: High Visible Light Photocatalytic Activity for Efficient Mineralization of Rhodamine B. Advanced Materials Interfaces, 2017, 4, 1700128.	3.7	44
80	Synthesis and evaluation of a novel chiral derivatization reagent for resolution of carboxylic acid enantiomers by RP-HPLC. Microchemical Journal, 2017, 135, 213-220.	4.5	15
81	Highly selective fluorescent probe based on new coordinated cationic polyvinylpyrrolidone for hydrogen sulfide sensing in aqueous solution. Journal of Molecular Liquids, 2017, 247, 35-42.	4.9	14
82	A Novel Copper Complex of Prolineâ€Based Mono(phenol) Amine Ligand (Hl <sup>pro</sup> ) Immobilized in SBAâ€15 as a Model Catalyst of Galactose Oxidase. ChemistrySelect, 2017, 2, 11164-11171.	1.5	4
83	Phospholipase A2-Responsive Phosphate Micelle-Loaded UCNPs for Bioimaging of Prostate Cancer Cells. Scientific Reports, 2017, 7, 16073.	3.3	39
84	Photocatalysis: A Mixedâ€Metal Oxides/Graphitic Carbon Nitride: High Visible Light Photocatalytic Activity for Efficient Mineralization of Rhodamine B (Adv. Mater. Interfaces 12/2017). Advanced Materials Interfaces, 2017, 4, .	3.7	0
85	Synthesis and characterization of an iron(III) complex of an ethylenediamine derivative of an aminophenol ligand in relevance to catechol dioxygenase active site. Polyhedron, 2017, 122, 116-123.	2.2	2
86	SYNTHESIS, CHARACTERIZATION, LUMINESCENCE AND DNA BINDING PROPERTIES OF Ln (III)-SCHIFF BASE FAMILY. Journal of the Chilean Chemical Society, 2017, 62, 3447-3453.	1.2	15
87	Derivatization reaction-based surface-enhanced Raman scattering (SERS) for detection of trace acetone. Talanta, 2016, 155, 87-93.	5.5	15
88	Facile Synthesis and Enantioseparation of Chiral Drugs Using Zirconia Magnetic Microspheres Coated with Cyclodextrin/Poly(amidoamine) Dendrimers. Bulletin of the Korean Chemical Society, 2016, 37, 1393-1394.	1.9	1
89	Tetrabromocatecholato Mn(III) complexes of bis(phenol) diamine ligands as models for enzyme–substrate adducts of catechol dioxygenases. Polyhedron, 2016, 118, 171-179.	2.2	4
90	Highly sensitive derivatization reagents possessing positively charged structures for the determination of oligosaccharides in glycoproteins by high-performance liquid chromatography electrospray ionization tandem mass spectrometry. Journal of Chromatography A, 2016, 1465, 79-89.	3.7	10

#	Article	IF	CITATIONS
91	A bright yellow light from a Yb <sup>3+</sup> ,Er <sup>3+</sup> -co-doped Y <sub>2</sub> SiO <sub>5</sub> upconversion luminescence material. RSC Advances, 2016, 6, 92454-92462.	3.6	24
92	Metabolic Isotope Labeling of Polysaccharides with Isotopic Glucose for Quantitative Glycomics in Cell Culture. Bulletin of the Korean Chemical Society, 2016, 37, 1518-1521.	1.9	5
93	CuO-Decorated ZnO Hierarchical Nanostructures as Efficient and Established Sensing Materials for H2S Gas Sensors. Scientific Reports, 2016, 6, 26736.	3.3	144
94	Fabrication of Two-Dimensional Arrays of Diameter-Tunable PS- <i>b</i> -P2VP Nanowires at the Air/Water Interface. Langmuir, 2016, 32, 11819-11826.	3.5	5
95	An improved non-enzymatic hydrogen peroxide sensor based on europium functionalized inorganic hybrid material—Evaluation of optical and electrochemical properties. Sensors and Actuators B: Chemical, 2016, 237, 81-89.	7.8	11
96	Preface to the special issue: Nanopia 2015. Applied Spectroscopy Reviews, 2016, 51, 513-516.	6.7	0
97	Pectin/poly(acrylamide- <i>co</i> -acrylamidoglycolic acid) pH sensitive semi-IPN hydrogels: selective removal of Cu <sup>2+</sup> and Ni <sup>2+</sup> , modeling, and kinetic studies. Desalination and Water Treatment, 2016, 57, 6503-6514.	1.0	28
98	Recent advances in luminescence properties of lanthanide-doped up-conversion nanocrystals and applications for bio-imaging, drug delivery, and optosensing. Applied Spectroscopy Reviews, 2016, 51, 678-705.	6.7	49
99	Influence of gold species (AuCl <sub>4</sub> <sup>â^'</sup> and AuCl <sub>2</sub> <sup>â^'</sup> ) on self-assembly of PS-b-P2VP in solutions and morphology of composite thin films fabricated at the air/liquid interfaces. Physical Chemistry Chemical Physics, 2016, 18, 1945-1952.	2.8	7
100	Adsorption and photodegradation kinetics of herbicide 2,4,5-trichlorophenoxyacetic acid with MgFeTi layered double hydroxides. Chemosphere, 2016, 146, 51-59.	8.2	42
101	TEMPO-mediated aerobic oxidation of alcohols using copper(II) complex of bis(phenol) di-amine ligand as biomimetic model for Galactose oxidase enzyme. Polyhedron, 2016, 106, 153-162.	2.2	16
102	Quantitative determination of uric acid using CdTe nanoparticles as fluorescence probes. Biosensors and Bioelectronics, 2016, 77, 359-365.	10.1	115
103	Upconversion fluorescence resonance energy transfer—a novel approach for sensitive detection of fluoroquinolones in water samples. Microchemical Journal, 2016, 124, 181-187.	4.5	34
104	Fabrication of a Selective and Sensitive Sensor Based on Molecularly Imprinted Polymer/Acetylene Black for the Determination of Azithromycin in Pharmaceuticals and Biological Samples. PLoS ONE, 2016, 11, e0147002.	2.5	20
105	Analysis of Benzanthrone in Urban Surface Soil Using Laser Desorption/Ferric Chloride Chemical Ionization Timeâ€ofâ€Flight Mass Spectrometry. Bulletin of the Korean Chemical Society, 2015, 36, 2750-2752.	1.9	2
106	Selective Detection of Hg <sup>2+</sup> lon Using Upconversion Luminescent Nanoparticles. Bulletin of the Korean Chemical Society, 2015, 36, 1307-1308.	1.9	12
107	Photochemical vapor generation and in situ preconcentration for determination of mercury by graphite furnace atomic absorption spectrometry. Analytical Methods, 2015, 7, 3015-3021.	2.7	30
108	Highly fluorescent CdTe quantum dots with reduced cytotoxicity-A Robust biomarker. Sensing and Bio-Sensing Research, 2015, 3, 46-52.	4.2	36

#	Article	IF	CITATIONS
109	Sensitive detection of bisphenol A in complex samples by in-column molecularly imprinted solid-phase extraction coupled with capillary electrophoresis. Microchemical Journal, 2015, 121, 1-5.	4.5	81
110	Rapid and selective extraction of multiple macrolide antibiotics in foodstuff samples based on magnetic molecularly imprinted polymers. Talanta, 2015, 137, 1-10.	5.5	82
111	Unique self-assembly behavior of amphiphilic block copolymers at liquid/liquid interfaces. RSC Advances, 2015, 5, 4334-4342.	3.6	15
112	New highly efficient electrochemical synthesis of dispersed Ag <sub>2</sub> O particles in the vicinity of the cathode with controllable size and shape. Journal of Materials Chemistry C, 2015, 3, 7720-7726.	5.5	22
113	Dielectric barrier discharge-assisted one-pot synthesis of carbon quantum dots as fluorescent probes for selective and sensitive detection of hydrogen peroxide and glucose. Talanta, 2015, 142, 51-56.	5.5	49
114	Iron(III) complex of N-phenylethylenediamine derivative of amine bis(phenol) ligand as model for catechol dioxygenase: Synthesis, characterization and complexation studies. Journal of Molecular Structure, 2015, 1094, 130-136.	3.6	3
115	A new strategy to fabricate composite thin films with tunable micro- and nanostructures via self-assembly of block copolymers. Chemical Communications, 2015, 51, 16687-16690.	4.1	20
116	A new and facile way to fabricate catalytically active block copolymer/Au nanoparticle multilayer thin films at the air/liquid interface. RSC Advances, 2015, 5, 86564-86571.	3.6	9
117	H:ZnO Nanorod-Based Photoanode Sensitized by CdS and Carbon Quantum Dots for Photoelectrochemical Water Splitting. Journal of Physical Chemistry C, 2015, 119, 24323-24331.	3.1	65
118	Fabrication of porous thin films of block copolymer at the liquid/liquid interface and construction of composite films doped with noble metal nanoparticles. RSC Advances, 2015, 5, 69339-69347.	3.6	7
119	Novel dithiols as capping ligands for CdSe quantum dots: optical properties and solar cell applications. Journal of Materials Chemistry C, 2015, 3, 1957-1964.	5.5	36
120	Emulsion-directed liquid/liquid interfacial fabrication of lanthanide ion-doped block copolymer composite thin films. Journal of Colloid and Interface Science, 2015, 438, 212-219.	9.4	5
121	(S)-1-methyl-4-(5-(3-aminopyrrolidin-1-yl)-2,4-dinitrophenyl)piperazine as a novel chiral derivatization reagent for high-performance liquid chromatographic analysis of carboxylic acid enantiomers. Microchemical Journal, 2015, 118, 176-182.	4.5	5
122	Controllable Synthesis of Thiol-Capped CdTe Nanoparticles for Optical Sensing of Triethylenetetramine Dihydrochloride. Journal of Nanoscience and Nanotechnology, 2014, 14, 7662-7667.	0.9	4
123	Determination of reduced glutathione, cystein and total thiols in pine pollen powder by in situ derivatization. Microchemical Journal, 2014, 112, 1-6.	4.5	7
124	Selective and sensitive determination of erythromycin in honey and dairy products by molecularly imprinted polymers based electrochemical sensor. Microchemical Journal, 2014, 116, 183-190.	4.5	47
125	Synthesis and photoluminescence of Cr-, Ni-, Co-, and Ti-doped ZnSe nanoparticles. Journal of Alloys and Compounds, 2014, 588, 127-132.	5.5	23
126	Facile synthesis of highly luminescent Mg(II), Cu(I)-codoped CdS/ZnSe core/shell nanoparticles. Chemical Engineering Journal, 2014, 236, 75-81.	12.7	25

#	Article	IF	CITATIONS
127	Polymorphs and dielectric properties of BaTi1â^'Ni O3. Journal of Alloys and Compounds, 2014, 583, 237-243.	5.5	16
128	Liquid/Liquid Interfacial Fabrication of Thermosensitive and Catalytically Active Ag Nanoparticle-Doped Block Copolymer Composite Foam Films. Langmuir, 2014, 30, 10503-10512.	3.5	23
129	Fabrication of Composite Polymer Foam Films at the Liquid/Liquid Interface through Emulsion-Directed Assembly and Adsorption Processes. Langmuir, 2014, 30, 2178-2187.	3.5	19
130	Isomeric quantification of O-diglycosyl flavonoids by a complex-free kinetic method using ESI/QToF mass spectrometry. Microchemical Journal, 2014, 117, 46-51.	4.5	4
131	Synthesis and properties of hemifluorinated disodium alkanesulfonates. Journal of Fluorine Chemistry, 2014, 163, 42-45.	1.7	11
132	Unique self-assembly behavior of a triblock copolymer and fabrication of catalytically active gold nanoparticle/polymer thin films at the liquid/liquid interface. Materials Chemistry and Physics, 2014, 146, 88-98.	4.0	9
133	Selective optosensing of clenbuterol and melamine using molecularly imprinted polymer-capped CdTe quantum dots. Biosensors and Bioelectronics, 2014, 57, 310-316.	10.1	129
134	Synthesis and Catalytic Applications of Ruthenium(0) Nanoparticles in Click Chemistry. Bulletin of the Korean Chemical Society, 2014, 35, 1144-1148.	1.9	17
135	Dual Responsive Pectin Hydrogels and Their Silver Nanocomposites: Swelling Studies, Controlled Drug Delivery and Antimicrobial Applications. Bulletin of the Korean Chemical Society, 2014, 35, 2391-2399.	1.9	27
136	Stimuli-Sensitive Poly(NIPA-co-APA) Hydrogels for the Controlled Release of Keterolac Tromethamine. Journal of the Korean Chemical Society, 2014, 58, 92-99.	0.2	3
137	Poly [2-(cinnamoyloxy)ethyl methacrylate-co-octamethacryl-POSS] nanocomposites: Synthesis and properties. Reactive and Functional Polymers, 2013, 73, 1175-1179.	4.1	8
138	Structural, magnetic, infrared and Raman studies of La0.8Sr x Ca0.2-x MnO3 (0Ââ‰ÂxÂâ‰Â0.2). Journal of Materials Science: Materials in Electronics, 2013, 24, 2292-2301.	2.2	32
139	Chiral zirconia magnetic microspheres as a new recyclable selector for the discrimination of racemic drugs. Journal of Materials Chemistry B, 2013, 1, 4909.	5.8	40
140	LED-induced in-column molecular imprinting for solid phase extraction/capillary electrophoresis. Analyst, The, 2013, 138, 2821.	3.5	19
141	Preparation of palladium nanoparticles on alumina surface by chemical co-precipitation method and catalytic applications. Applied Surface Science, 2013, 265, 500-509.	6.1	47
142	Free-standing poly(2-vinylpyridine) foam films doped with silver nanoparticles formed at the planar liquid/liquid interface. Journal of Colloid and Interface Science, 2013, 394, 223-230.	9.4	24
143	Interfacial assembly of Pt nanoparticle-doped free-standing polymer foam films and their catalytic performance. Colloids and Surfaces A: Physicochemical and Engineering Aspects, 2013, 419, 201-208.	4.7	12
144	Optical properties and Judd–Ofelt parameters of Dy3+ doped K2GdF5 single crystal. Optical Materials, 2013, 35, 1636-1641.	3.6	46

#	Article	IF	CITATIONS
145	Fabrication of composite thin films with microstructures of honeycomb, foam, and nanosphere arrays through adsorption and self-assembly of block copolymers at the liquid/liquid interface. Journal of Colloid and Interface Science, 2013, 407, 225-235.	9.4	17
146	A novel colorimetric and fluorescent sensor for fluoride and pyrophosphate based on fluorenone signaling units. Microchemical Journal, 2013, 106, 27-33.	4.5	23
147	Isolation and characterization of BTEX tolerant and degrading Pseudomonas putida BCNU 106. Biotechnology and Bioprocess Engineering, 2013, 18, 1000-1007.	2.6	18
148	Determination of the polyamines in human toenails as 1-(5-fluoro-2,4-dinitrophenyl)-4-methylpiperazine derivatives using high-performance liquid chromatography. Microchemical Journal, 2013, 110, 568-574.	4.5	6
149	Terpene Alcohols InhibitDe NovoSphingolipid Biosynthesis. Planta Medica, 2012, 78, 434-439.	1.3	3
150	Microwave-enhanced cold vapor generation for speciation analysis of mercury by atomic fluorescence spectrometry. Talanta, 2012, 94, 146-151.	5.5	41
151	Molecularly imprinted solid phase microextraction fiber for trace analysis of catecholamines in urine and serum samples by capillary electrophoresis. Talanta, 2012, 99, 270-276.	5.5	67
152	A new iron(III) complex of glycine derivative of amine-chloro substituted phenol ligand: Synthesis, characterization and catechol dioxygenase activity. Journal of Molecular Structure, 2012, 1029, 60-67.	3.6	22
153	Judd–Ofelt analysis of spectroscopic properties of Sm3+ ions in K2YF5 crystal. Journal of Alloys and Compounds, 2012, 520, 262-265.	5.5	67
154	Electrical properties of BiFeO3 and (Bi0.9Eu0.1)(Fe0.9Mn0.1)O3â^î^î thin films. Journal of the Korean Physical Society, 2012, 60, 193-197.	0.7	1
155	Ultrasensitive determination of cobalt and nickel by atomic fluorescence spectrometry using APDC enhanced chemical vapor generation. Microchemical Journal, 2012, 104, 33-37.	4.5	34
156	Broad-spectrum In vitro antimicrobial activities of Streptomyces sp. strain BCNU 1001. Biotechnology and Bioprocess Engineering, 2012, 17, 576-583.	2.6	7
157	Synthesis and characterization of chitosan–PEG–Ag nanocomposites for antimicrobial application. Carbohydrate Polymers, 2012, 87, 920-925.	10.2	96
158	One-step synthesis and assembly of one-dimensional parallel chains of CdS nanoparticles at the air–water interface templated by 10,12-pentacosadiynoic acid supermolecules. Journal of Colloid and Interface Science, 2012, 375, 118-124.	9.4	7
159	Nano TiO2-based preconcentration for the speciation analysis of inorganic selenium by using ion chromatography with conductivity detection. Microchemical Journal, 2012, 101, 70-74.	4.5	22
160	Simple mercury speciation analysis by CVG-ICP-MS following TMAH pre-treatment and microwave-assisted digestion. Microchemical Journal, 2012, 103, 105-109.	4.5	28
161	On-line chiral analysis of benzylmercapturic acid and phenylmercapturic acid in human urine using UPLC-QToF mass spectrometry with the kinetic method. Microchemical Journal, 2012, 103, 170-176.	4.5	6
162	Fabrication of Amino Acid Based Silver Nanocomposite Hydrogels from PVA- Poly(Acrylamide-co-Acryloyl phenylalanine) and Their Antimicrobial Studies. Bulletin of the Korean Chemical Society, 2012, 33, 3191-3195.	1.9	10

#	Article	IF	CITATIONS
163	Formation of Ag Nanoparticle-Doped Foam-like Polymer Films at the Liquid–Liquid Interface. Journal of Physical Chemistry B, 2011, 115, 11113-11118.	2.6	25
164	Reduction of Eu3+ to Eu2+ in NaCaPO4:Eu phosphors prepared in a non-reducing atmosphere. Journal of Alloys and Compounds, 2011, 509, 7937-7942.	5.5	73
165	Differentiation of cis- and trans-isomers of the novel napthalene-aza receptor by naked-eye colorimetric anion sensing. Tetrahedron Letters, 2011, 52, 6465-6469.	1.4	10
166	Gold hierarchical nanostructures formed at the solid/liquid interfaces via electroless deposition and their SERS properties. Colloids and Surfaces A: Physicochemical and Engineering Aspects, 2011, 387, 1-9.	4.7	4
167	Synthesis and assembly of catalytically active platinum-doped polymer nanocomposites at the liquid/liquid interface. Colloids and Surfaces A: Physicochemical and Engineering Aspects, 2011, 386, 141-141.	4.7	14
168	Synthesis and luminescence properties of cinnamide based nanohybrid materials containing Eu (II) ions. Journal of Crystal Growth, 2011, 326, 128-134.	1.5	1
169	Development of novel active acceptors possessing a positively charged structure for the transglycosylation reaction with Endo-M and their application to oligosaccharide analysis. Rapid Communications in Mass Spectrometry, 2011, 25, 2911-2922.	1.5	3
170	Nanoplates and nanostars of β-PbO formed at the air/water interface. Colloids and Surfaces A: Physicochemical and Engineering Aspects, 2011, 373, 124-129.	4.7	36
171	Rapid and selective determination of urinary lysozyme based on magnetic molecularly imprinted polymers extraction followed by chemiluminescence detection. Analytica Chimica Acta, 2011, 692, 73-79.	5.4	54
172	Synthesis, crystal structure, magnetic and redox properties of copper(II) complexes of N-alkyl(aryl) tBu-salicylaldimines. Inorganica Chimica Acta, 2011, 366, 275-282.	2.4	26
173	Determination of trace bisphenol A in complex samples using selective molecularly imprinted solid-phase extraction coupled with capillary electrophoresis. Microchemical Journal, 2011, 98, 150-155.	4.5	94
174	Mechanistic study on the effect of PEG molecules in a trivalent chromium electrodeposition process. Microchemical Journal, 2011, 99, 7-14.	4.5	36
175	Luminescent properties of a new green emitting Eu2+ doped CaZrSi2O7 phosphor for WLED applications. Journal of Luminescence, 2011, 131, 2414-2418.	3.1	32
176	Synthesis and assembly of gold nanoparticle-doped polymer solid foam films at the liquid/liquid interface and their catalytic properties. Journal of Colloid and Interface Science, 2011, 362, 81-88.	9.4	40
177	Non-Extractive Simultaneous Spectrophotometric Determination of Trace Quantities of Palladium(II) and Tungsten(VI). Analytical Letters, 2011, 44, 815-823.	1.8	5
178	A Systematic Study on Preparing the CdS Quantum Dots. Journal of the Korean Physical Society, 2011, 59, 3293-3299.	0.7	12
179	Application of the Judd ? Ofelt Theory to Dy3+-Doped Fluoroborate/Sulphate Glasses. Journal of the Korean Physical Society, 2011, 59, 3300-3307.	0.7	16
180	Synthesis, Characterization, and Antibacterial Applications of Novel Copolymeric Silver Nanocomposite Hydrogels. Bulletin of the Korean Chemical Society, 2011, 32, 553-558.	1.9	29

#	Article	IF	CITATIONS
181	Preparation and characterization of nifedipine-loaded cellulose acetate butyrate based microspheres and their controlled release behavior. Polymer Bulletin, 2010, 65, 157-167.	3.3	9
182	Development of semi-interpenetrating carbohydrate polymeric hydrogels embedded silver nanoparticles and its facile studies on E. coli. Carbohydrate Polymers, 2010, 81, 196-202.	10.2	53
183	Single-Pair Fluorescence Resonance Energy Transfer (spFRET) for the High Sensitivity Analysis of Low-Abundance Proteins Using Aptamers as Molecular Recognition Elements. Journal of Fluorescence, 2010, 20, 203-213.	2.5	12
184	Poly(9â€vinylcarbazole)/silver composite nanotubes and networks formed at the air–water interface. Journal of Applied Polymer Science, 2010, 116, 252-257.	2.6	135
185	Isomeric discrimination and quantification of thyroid hormones, T <sub>3</sub> and rT <sub>3</sub> , by the single ratio kinetic method using electrospray ionization mass spectrometry. Journal of the American Society for Mass Spectrometry, 2010, 21, 14-22.	2.8	13
186	Trace analysis of tetracycline antibiotics in human urine using UPLC–QToF mass spectrometry. Microchemical Journal, 2010, 94, 139-147.	4.5	49
187	Determination of R-(+)-higenamine enantiomer in Nelumbo nucifera by high-performance liquid chromatography with a fluorescent chiral tagging reagent. Microchemical Journal, 2010, 96, 374-379.	4.5	24
188	Antibacterial and luminescent properties of new donor–acceptor ruthenium triphenylphosphine–bipyridinium complexes. Microchemical Journal, 2010, 95, 235-239.	4.5	7
189	Fluorescence Spectroscopy of Polymer Systems Doped with Rare-Earth Metal Ions and Their Complexes. Applied Spectroscopy Reviews, 2010, 45, 409-446.	6.7	24
190	Cross-Talk-Free Dual-Color Fluorescence Cross-Correlation Spectroscopy for the Study of Enzyme Activity. Analytical Chemistry, 2010, 82, 1401-1410.	6.5	16
191	A Simple and Convenient Synthesis of (±)-Methylcyclopentanone-3-carboxylate; an Important Precursor of Antitumor Drug Sarkomycin. Bulletin of the Korean Chemical Society, 2010, 31, 1732-1734.	1.9	1
192	Preparation and Characterization of Porous and Composite Nanoparticulate Films of CdS at the Air/Water Interface. Bulletin of the Korean Chemical Society, 2010, 31, 2547-2552.	1.9	0
193	Silver nanoplates formed at the air/water and solid/water interfaces. Colloids and Surfaces A: Physicochemical and Engineering Aspects, 2009, 340, 93-98.	4.7	19
194	Detoxification of Cytotoxic Alachlor by Glutathione: Characterization of Conjugated Adducts by Electrospray Ionization Tandem Mass Spectrometry. Journal of Agricultural and Food Chemistry, 2009, 57, 9838-9847.	5.2	4
195	Recent Development on Spectroscopic Methods for Chiral Analysis of Enantiomeric Compounds. Applied Spectroscopy Reviews, 2009, 44, 267-316.	6.7	36
196	Kinetic method for enantiomeric determination of thyroid hormone (d,l-thyroxine) using electrospray ionization tandem mass spectrometry (ESI-MS/MS). International Journal of Mass Spectrometry, 2008, 272, 180-186.	1.5	22
197	Semi-IPN hydrogels based on Poly(vinyl alcohol) for controlled release studies of chemotherapeutic agent and their Swelling characteristics. Polymer Bulletin, 2008, 61, 81-90.	3.3	31
198	Determination of enantiomeric compositions of DOPA by tandem mass spectrometry using the kinetic method with fixed ligands. Rapid Communications in Mass Spectrometry, 2008, 22, 909-915.	1.5	26

#	Article	IF	CITATIONS
199	Gold and silver nanorings formed at the air/water interface. Colloids and Surfaces A: Physicochemical and Engineering Aspects, 2008, 312, 203-208.	4.7	19
200	Determination of thyroxine enantiomers in pharmaceutical formulation by high-performance liquid chromatography–mass spectrometry with precolumn derivatization. Microchemical Journal, 2008, 88, 62-66.	4.5	24
201	Triangular PbS Nano-Pyramids, Square Nanoplates, and Nanorods Formed at the Air/Water Interface. Crystal Growth and Design, 2008, 8, 2660-2664.	3.0	23
202	One-step synthesis of silver nanoparticles at the air–water interface using different methods. Nanotechnology, 2008, 19, 055603.	2.6	7
203	Interaction of Glutathione and Sodium Selenite In vitro Investigated by Electrospray Ionization Tandem Mass Spectrometry. Journal of Biochemistry, 2008, 143, 685-693.	1.7	22
204	Investigation on C <sub>2</sub> -Ceramide Complexes with Transition Metal Ions Using Electrospray Ionization Tandem Mass Spectrometry. European Journal of Mass Spectrometry, 2008, 14, 87-97.	1.0	5
205	Enhanced Detection and Structural Characterization of Flavonoids by Complexation with N,O-Bis(trimethysilyl)trifluoroacetamide Using Electrospray Ionization Mass Spectrometry. Analytical Sciences, 2008, 24, 1177-1182.	1.6	6
206	Investigation of the Interaction Between Sodium (meta) Arsenite and Catechin via ESI Tandem Mass Spectrometry. Chemical Research in Chinese Universities, 2007, 23, 524-529.	2.6	2
207	Synthesis and assembly of ordered nanostructures of ZnS, Zn <sub><i>x</i></sub> Cd <sub>1â^'<i>x</i></sub> S and CdS nanoparticles at the air/water interface. Nanotechnology, 2007, 18, 435603.	2.6	17
208	Enantioselective resolution of thyroxine hormone by high-performance liquid chromatography utilizing a highly fluorescent chiral tagging reagent. Chirality, 2007, 19, 625-631.	2.6	8
209	Enhancement of the detection sensitivity for volatile organic compounds by using an annular type photoionization detector and a pre-concentration system. Analytica Chimica Acta, 2007, 583, 210-215.	5.4	5
210	Structural characterization of alachlor complexes with transition metal ions by electrospray ionization tandem mass spectrometry. Microchemical Journal, 2007, 86, 248-256.	4.5	3
211	Influences of compositions and ligands on photoluminescent properties of Eu(III) ions in composite europium complex/PMMA systems. Journal of Luminescence, 2007, 127, 307-315.	3.1	19
212	Synthesis of one-dimensional silver oxide nanoparticle arrays and silver nanorods templated by Langmuir monolayers. Journal of Colloid and Interface Science, 2007, 314, 297-303.	9.4	25
213	Optical Hole-Burning Properties of Sm2+-Doped Strontium Borates. Journal of the Physical Society of Japan, 2006, 75, 054709.	1.6	3
214	Determination of pKa value, kinetic studies of decomposition and oxygen transfer for chromium(VI) peroxide. Microchemical Journal, 2006, 82, 73-77.	4.5	6
215	The mechanism of photobleaching in Sm2+-doped alkaline-earth fluorohalides. Journal of Luminescence, 2005, 113, 9-16.	3.1	11
216	Influences of matrices and concentrations on luminescent characteristics of Eu(TTA)3(H2O)2/polymer composites. Journal of Luminescence, 2005, 114, 187-196.	3.1	16

#	Article	IF	CITATIONS
217	Ferroelectric properties of lanthanum-doped bismuth titanate thin films grown by a sol–gel method. Thin Solid Films, 2005, 472, 90-95.	1.8	56
218	Novel luminescent Langmuir–Blodgett films of europium complex embedded in titania matrix. Thin Solid Films, 2005, 491, 217-220.	1.8	9
219	Studies on photoluminescent properties of Eu(III) ions in composite europium complex/polymer systems. Colloids and Surfaces A: Physicochemical and Engineering Aspects, 2005, 257-258, 301-305.	4.7	9
220	Influence of Sm3+-Ions on the Hole-Burning Efficiency of Sm2+-Ions Doped in Mg0.5Sr0.5FCl0.5Br0.5Mixed Crystals. Japanese Journal of Applied Physics, 2004, 43, 8103-8106.	1.5	2
221	The influence of metal aluminium on the reduction of the Sm3+doped in aluminosilicate glass films. Journal of Physics Condensed Matter, 2004, 16, 2543-2549.	1.8	9
222	Effects of Donor Ion Doping on the Orientation and Ferroelectric Properties of Bismuth Titanate Thin Films. Japanese Journal of Applied Physics, 2004, 43, 237-241.	1.5	33
223	Optical properties of Tm-doped GaSe single crystals. Solid State Communications, 2004, 130, 701-704.	1.9	13
224	Photophysical properties of a conjugated poly(1-dodecyl-2,5-pyrrylene vinylene). Macromolecular Research, 2004, 12, 322-324.	2.4	1
225	Influence of ligands on the photoluminescent properties of Eu3+ in europium β-diketonate/PMMA-doped systems. Journal of Luminescence, 2004, 106, 47-55.	3.1	39
226	Distinct composite structure and properties of Eu(phen)2Cl3(H2O)2 in poly(methyl methacrylate) and polyvinylpyrrolidone. Journal of Applied Polymer Science, 2004, 92, 3524-3530.	2.6	27
227	Photoluminescent behaviors of several kinds of europium ternary complexes doped in PMMA. Journal of Luminescence, 2004, 110, 11-16.	3.1	59
228	Ferroelectric Bi3.4Eu0.6Ti3O12 thin films deposited on Si(100) and Pt/Ti/SiO2/Si(100) substrates by a sol–gel process. Journal of Crystal Growth, 2004, 262, 327-333.	1.5	19
229	Electrical properties of samarium-substituted Bi4Ti3O12 thin films grown on p-type Si substrates. Journal of Crystal Growth, 2004, 268, 204-209.	1.5	4
230	Analytical evaluation of electrothermal vaporization/low-pressure inductively coupled plasma atomic emission spectrometry for trace elemental analysis in microliter samples. Microchemical Journal, 2004, 78, 127-134.	4.5	2
231	Studies on composites formed by europium complexes with different ligands and polyvinylpyrrolidone. Materials Letters, 2004, 58, 1677-1682.	2.6	20
232	Different photoluminescent properties of binary and ternary europium chelates doped in PMMA. Materials Chemistry and Physics, 2003, 82, 84-92.	4.0	39
233	Influence of molecular structures of europium bisphthalocyanines on organization of supramolecular assemblies formed at the air/water interface. Materials Science and Engineering C, 2003, 23, 501-507.	7.3	11
234	Influences of hydrophilic and hydrophobic substituents on the organization of supramolecular assemblies of porphyrin derivatives formed at the air/water interface. Materials Science and Engineering C, 2003, 23, 585-592.	7.3	26

#	Article	IF	CITATIONS
235	Determination of trace cobalt in fruit samples by resonance ionization mass spectrometry. Microchemical Journal, 2003, 75, 87-96.	4.5	11
236	Supramolecular assemblies of Eu(TPyP)Pc at the air/water and air/Cd2+ aqueous solution interfaces. Materials Letters, 2003, 57, 2156-2161.	2.6	16
237	RECENT DEVELOPMENTS IN INSTRUMENTATION FOR LASER INDUCED BREAKDOWN SPECTROSCOPY. Applied Spectroscopy Reviews, 2002, 37, 89-117.	6.7	80
238	Direct Determination of Strontium in Marine Algae Samples by Laser-Induced Breakdown Spectrometry. Applied Spectroscopy, 2002, 56, 1511-1514.	2.2	15
239	Characterization of single-stranded DNA separation by capillary gel electrophoresis. Microchemical Journal, 2002, 72, 305-313.	4.5	5
240	Recent Developments in Laser-induced Breakdown Spectrometry. ISIJ International, 2002, 42, S129-S136.	1.4	15
241	Chapter 6 Laser-induced breakdown spectrometry: potential in biological and clinical samples. Advances in Atomic Spectroscopy, 2002, , 287-360.	0.8	0
242	Application of laser-induced breakdown spectrometry for direct determination of trace elements in starch-based flours. Journal of Analytical Atomic Spectrometry, 2001, 16, 622-627.	3.0	54
243	Solvent sublation using 8-hydroxyquinoline as a ligand for determination of trace elements in water samples. Microchemical Journal, 2001, 68, 99-107.	4.5	26
244	Extraction of palladium metal from aqueous solution of palladium chloride by laser-induced photochemistry. Microchemical Journal, 2001, 68, 121-126.	4.5	10
245	Spatially resolved elemental analysis of a hydrogen–air diffusion flame by laser-induced plasma spectroscopy (LIPS). Microchemical Journal, 2001, 70, 143-152.	4.5	11
246	A chelating resin containing 1-(2-thiazolylazo)-2-naphthol as the functional group; synthesis and sorption behavior for trace metal ions. Microchemical Journal, 2001, 70, 195-203.	4.5	50
247	Application of laser-induced breakdown spectrometry in urban health. Microchemical Journal, 2000, 67, 201-205.	4.5	6
248	Development and Characterization of Directly Connected Laser Ablation/Low-Pressure Inductively Coupled Plasma Atomic Emission Spectrometry for Solid Sample Analysis. Applied Spectroscopy, 2000, 54, 1253-1260.	2.2	7
249	Investigation of the Line-Broadening Mechanism for Laser-Induced Copper Plasma by Time-Resolved Laser-Induced Breakdown Spectroscopy. Microchemical Journal, 1999, 63, 53-60.	4.5	22
250	Novel and Recent Applications of Elemental Determination by Laser-Induced Breakdown Spectrometry. Analytical Letters, 1999, 32, 2143-2162.	1.8	88
251	Laser-induced breakdown spectrometry. Advances in Atomic Spectroscopy, 1999, , 235-288.	0.8	5
252	New Calix[4]arene Dibenzocrown Ethers for Selective Sensing of Cesium Ion in an Aqueous Environment. Microchemical Journal, 1998, 58, 225-235.	4.5	19

#	Article	IF	CITATIONS
253	Potassium Sensing Calix[4]arene Crown Ethers. Microchemical Journal, 1998, 59, 464-471.	4.5	24
254	Design and Critical Evaluation of Improved Electrothermal Vaporization Flame Atomic Absorption/Emission Spectrometry for Direct Determination of Trace Metals in Microliter Samples. Microchemical Journal, 1998, 60, 231-241.	4.5	5
255	Laser-Induced Breakdown Spectrometry. The Chemical Educator, 1998, 3, 1-7.	0.0	12
256	Lasers in Analytical Atomic Spectrometry–An Overview1. Spectroscopy Letters, 1997, 30, 1417-1427.	1.0	11
257	Applications of Laser-Induced Breakdown Spectrometry. Applied Spectroscopy Reviews, 1997, 32, 183-235.	6.7	244
258	Influence of Atmosphere and Irradiation Wavelength on Copper Plasma Emission Induced by Excimer and Q-Switched Nd:YAG Laser Ablation. Applied Spectroscopy, 1997, 51, 959-964.	2.2	86
259	Investigation of the Metal Cation Binding Properties of Macrocyclic EDTA–Bis(Amide) Complexes by Potentiometry and Stopped-Flow Spectrophotometry. Microchemical Journal, 1997, 55, 357-366.	4.5	2
260	Synthesis of Lipophilic Acyclic Diionizable Polyethers and Selective Transport of Alkaline-Earth Cations in Bulk Liquid Membrane System. Microchemical Journal, 1997, 55, 115-121.	4.5	8
261	An improved impaction-graphite furnace system for the direct and near real-time determination of cadmium, chromium, lead and manganese in aerosols and cigarette smoke by simultaneous multielement atomic absorption spectrometry. Spectrochimica Acta, Part B: Atomic Spectroscopy, 1996, 51, 109-116.	2.9	18
262	Potentiometry of the Dioxa–Triaza Macrocyclic Complexes as Receptors for First-Row Transition and Lanthanide Metals. Microchemical Journal, 1996, 53, 180-187.	4.5	3
263	Liquid Chromatographic Separation and Indirect Detection of Azacrown Compounds Using α-Naphthalene Sulfonic Acid as a Detection Reagent. Microchemical Journal, 1996, 53, 454-460.	4.5	2
264	Formation kinetics of triaza-crown-alkanoic acid complexes of first-row transition metal(II) ions. Supramolecular Chemistry, 1996, 7, 27-31.	1.2	4
265	Direct and rapid determination of potassium in standard solid glasses by excimer laser ablation plasma atomic emission spectrometry. Analyst, The, 1994, 119, 1441.	3.5	31
266	Interaction of a Laser Beam with Metals. Part II: Space-Resolved Studies of Laser-Ablated Plasma Emission. Applied Spectroscopy, 1992, 46, 436-441.	2.2	90
267	Interaction of an Excimer-Laser Beam with Metals. Part III: The Effect of a Controlled Atmosphere in Laser-Ablated Plasma Emission. Applied Spectroscopy, 1992, 46, 1597-1604.	2.2	96
268	Lasers in atomic spectroscopy: Selected applications. Microchemical Journal, 1992, 45, 1-35.	4.5	29
269	Fiber-optic probe laser-induced breakdown spectrometry for remote detection of toxic elements. , 0, , .		1